ELSEVIER

International Journal of Mass Spectrometry 208 (2001) 147–157

International Journal of Mass Spectrometry

Behavior of excited $C_3H_6O^+$ cations: a He-Iα photoelectron-photoion coincidence study of propanal

Josef Dannacher*,[1], Jean-Pierre Stadelmann[2]

Physikalisch-Chemisches Institut der Universität Basel, Klingelbergstrasse 80, CH-4056 Basel, Switzerland

Received 9 January 2001; accepted 12 March 2001

Abstract

The breakdown diagram of propanal cation is reported. Relying on He-Iα photoelectron-photoion coincidence an excitation energy range of 7 eV has been probed and all the major fragment ions have been studied. The specific decay behavior of the title cation is characterized and related to our earlier data on other $C_3H_6O^+$ isomers. The results are in excellent accord with literature ab initio calculations in terms of the threshold rate and the height of the energy barrier of the least endothermic fragmentation. For low excitation energies, our data imply that propanal radical cation does at most negligibly isomerize to the most stable distonic ion. The lion's share of the detected $C_3H_5O^+$ daughter ions has the propanoyl structure irrespective of the internal energy of the parent ion precursor. It is this fact, in conjunction with the extended Franck-Condon gap in the pertinent energy range, that prevents $C_3H_5O^+$ from being the base peak in the mass spectrum of propanal. In the breakdown diagram of propanal, only the $C_2H_6^+$ breakdown curve is identical to its counterpart obtained when studying allyl alcohol and cyclopropanal in exactly the same way. Competitive formation of $C_2H_6^+$ cannot be accounted for by quasi-equilibrium theory calculations. Conceivable models to rationalize the corresponding dissociation involve an electronic predissociation and/or ion-neutral complexes. (Int J Mass Spectrom 208 (2001) 147–157) © 2001 Elsevier Science B.V.

Keywords: Propanal; Propanal cation; Photoelectron-photoion coincidence data; Quasi-equilibrium theory calculations

1. Introduction

One of the most dependable areas of research on fundamental processes is provided by work on radical cations. These studies furnish spectroscopic data [1] and thermochemical values [2], afford insight into the elementary reactions [3] and quantify the distribution and redistribution of the available energy among the individual degrees of freedom [4]. It is such results that let us firmly establish and extend the foundation of mass spectroscopy, a technique of unparalleled significance to chemistry.

Radiative and nonradiative relaxation pathways are both accessible to isolated excited radical cations in the gas phase [5]. The radiationless processes comprise the redistribution of the excitation energy [6], extensive isomerizations [7] as well as the proper dissociations. Altogether, in a complex interplay, these processes are mapped into the mass spectroscopic fragmentation pattern. As long as a simple

* To whom correspondence should be addressed. E-mail: josef.dannacher@cibasc.com

[1] Present address: CIBASC, P.O. Box 1266, Koechlinstrasse I, D-79630 Grenzach-Wyhlen, Germany.

[2] Present address: UBS AG, B.O. Box, CH-4002 Basel, Switzerland

Dedicated to Professor Edgar Heilbronner on the occasion of his 80th birthday

PII S1387-3806(01)00387-6

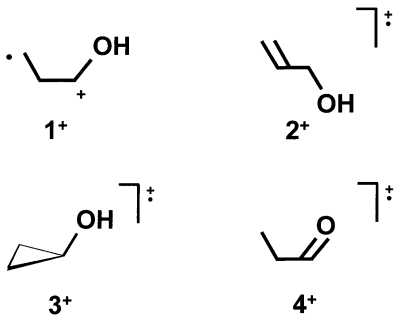

Scheme 1. Relevant $C_3H_6O^+$ isomers.

bond cleavage model and very few typical rearrangement reactions suffice to convincingly interpret a specific mass spectrum, chemists tend to ignore what happens backstage. However, missing peaks and unexpected signals in terms of *m/z* and/or relative intensity may make them change their mind.

$C_3H_6O^+$ ions have been extensively investigated during the last two decades [8–10]. As a model this system is of suitable size and complexity, i.e., sufficiently large to admit the cited processes and to be of practical relevance, but still adequately small to render high-quality ab initio calculations feasible. Outstanding theoretical work [9] of more recent date has located the most relevant stationary points of the potential energy surface and has characterized the most important transition states. The same study provided a good estimate regarding the energy profile of the least endothermic fragmentation reaction, corresponding to the formation of the propanoyl cation and a hydrogen atom. These computations are corroborated by a whole series of experimental data forthcoming from various techniques, such as metastable ion decomposition, collision-activated dissociation and neutralization-reionization mass spectroscopy [10]. More specifically, the distonic ion ($CH_2CH_2CHOH^+$; $\mathbf{1}^+$, cf. Scheme 1) has been demonstrated to be the common structure allyl alcohol **(2)** and cyclopropanol **(3)** isomerize to upon ionization [9,10]. The existence of such a common intermediate, at that time of unknown structure, was inferred from the identical breakdown diagrams of $\mathbf{2}^+$ and $\mathbf{3}^+$ as determined by He-Iα photoelectron-photoion coincidence (He-Iα PEPICO) spectroscopy [11]. Quite remarkably, this dissociative equivalence holds true for a whole range of excitation energies of more than 5 eV and for all the fragment ions worthy of note. On the other hand, computations [9] and experiments [10] clearly reveal a distinctly different behavior for ionized propanal ($\mathbf{4}^+$). Propanal cation essentially retains the structure of its neutral precursor for internal energies up to 0.66 eV. Also, a key role is assigned to $\mathbf{4}^+$ regarding the lowest energy fragmentation channel, i.e. formation of propanoyl cation and a hydrogen atom. The calculated energy profile along this reaction pathway [9], suggests a barrier of some 30 kJ/mol for the reverse reaction. Further, a threshold rate constant exceeding 10^8 s^{-1} is estimated by means of statistical calculations performed on the ab initio potential energy surface. Nearly all of the available experimental data [12,13] confirm the existence of such a barrier. The only noteworthy exception concerns a photoionization (PI) study of **4** where the dissociation in question was observed at its thermochemical limit [14]. Moreover, the estimated threshold rate [9] cannot account for the metastable transition reported in the literature [12].

To answer some of the remaining questions, we determined the breakdown diagram of excited $\mathbf{4}^+$ relying on He-Iα PEPICO spectroscopy. Working with one and the same spectrometer allows a straightforward comparison with our earlier data on other $C_3H_6O^+$ isomers [11,15]. An excitation energy range of some 7 eV was probed in the present case, and the most important fragment ions were studied. As to the least endothermic fragmentation, our data are in complete accord with the ab initio molecular orbital calculations [9]. Further aspects of the behavior of internal energy selected $\mathbf{4}^+$ are reported, and their mass spectroscopic significance is discussed.

2. Experimental

A commercial sample of propional (Fluka AG, Buchs, Switzerland; stated purity >98%) was purified by distillation. Its mass spectrum indicated no significant amounts of impurities.

The coincidence spectrometer and the evaluation

of the coincidence data have been described in detail in our earlier publications [16]. In brief, on effusing from a hypodermic needle, the sample gas is ionized by a collimated beam of He-Iα radiation ($h\nu$ = 21.22 eV). Photoelectrons and photoions are extracted by a constant electrostatic field of F_s = 2 V/cm applied to the ionization region. The photoelectrons are energy selected by means of a hemispherical analyzer equipped with suitable electron optics. The corresponding resolving power amounts to $E \approx 75$. The photoions are focused into a quadrupole mass spectrometer which provides unity mass resolution. The transmission coefficients were $f_e \approx 0.007$ for the photoelectrons and f_i (M^+, $m/z = 58$) ≈ 0.2 for thermal parent ions of $m/z = 58$, respectively.

The breakdown diagram of $\mathbf{4}^+$ has been obtained by appropriately normalizing the detected genuine coincidences between mass-selected photoions and energy-selected photoelectrons as a function of the ionization energy (IE) [16]. This procedure involves the scaling of the individual fragment ion breakdown curves with the measurable transmission coefficient for thermal molecular ions. Note that this is only a first order approximation. Its reliability can be deduced from the deviation of the sum curve from unity [16]. In the present case this deviation is large especially at high ionization energies. Consequently, our fragment ion branching ratios are merely lower bounds to the true values. Discrimination effects of the spectrometer against fragment ions of high translational energy are responsible for this deficiency.

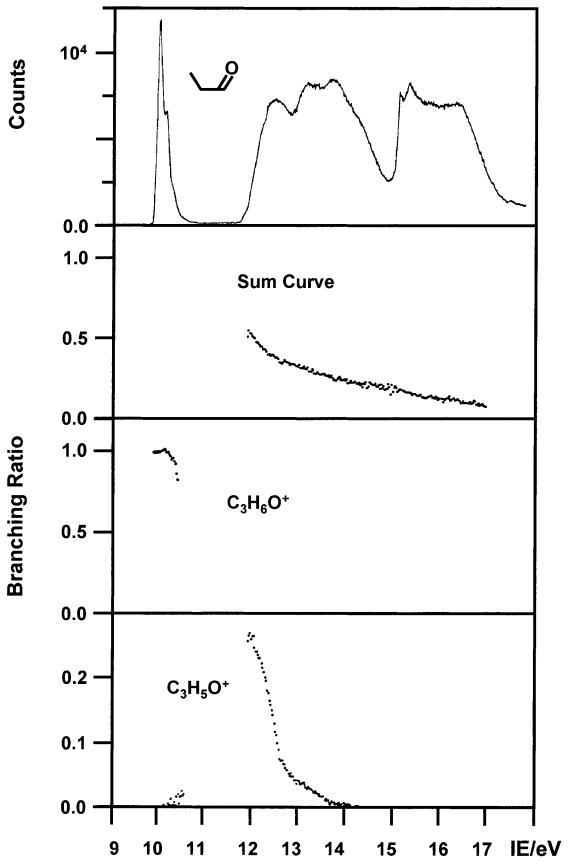

Fig. 1. Photoelectron spectrum of propanal as obtained under coincidence conditions. The sum curve and the breakdown curves for $C_3H_6O^+$ and $C_3H_5O^+$.

3. Results and discussion

3.1. Relevant aspects of the photoelectron spectrum

When operating in the coincidence mode, our spectrometer provides a photoelectron spectrum (PES) of propanal as shown in Fig. 1. Its major features of particular consequence to the present work are as follows. Removal of an electron of the oxygen lone pair yields propanal radical cations in the electronic ground state $\tilde{X}\ ^2A'$. With the maximum intensity at the 0–0 transition tantamount to an adiabatic ionization energy of IE_1^a = 9.98 eV (recommended literature value 9.96 eV [17]) and obvious vibrational fine structure, the nonbonding character of this orbital is confirmed. This implies that ground state parent cations essentially retain the structure of their neutral precursors, which is in accord with the outcome of collisional activation studies [10] and the quantum chemical computations [9]. Due to the reduced resolving power in the coincidence mode this fine structure becomes somewhat blurred. However, a vibrational spacing of some 0.16 eV, as detected under high resolution, is still discernible in Fig. 1. Unfavorable Franck-Condon factors oppose any noteworthy population of the $\tilde{X}\ ^2A'$ state for IE $\geq$ 10.6 eV. Below this energy there is only one accessible fragmentation

channel corresponding to loss of a hydrogen atom, yielding propanoyl fragment ions.

Above the Franck-Condon gap of $10.6 \leq IE \leq 11.9$ eV, population of various excited electronic states becomes feasible. The spectrum shows several overlapping bands with divers local maxima. As to the nature of the corresponding vacant molecular orbitals, the reader is referred to the assignment given in the high-resolution study [18].

In the present context, it is sufficient to point out that the first excited electronic state $\tilde{A}\,^2A''$ arises from ionization of the π orbital of the C=O double bond. The strongly bonding nature of this orbital is reflected by the band shape. Our vertical ionization energy is $IE_2^v \approx 12.5$ eV (high-resolution literature data advocate for 12.62 eV [18] or 12.4 eV [19], respectively), whereas our adiabatic value approximated by the onset of the band amounts to about 11.9 eV (literature value $IE_2^a = 11.88$ eV [20]).

3.2. Relevant aspects of the mass spectrum

The He-Iα photoionization mass spectra of allyl alcohol and propanal are listed in Table 1. High resolution electron impact (EI) data [21] on propanal are also given. They render it possible to estimate the relative contributions of oxygen-containing and hydrocarbon fragment ions of identical mass number. Notably, practically the total intensity observed at $m/z = 30$ and $m/z = 28$ stems from the oxygen free species, whereas the signal at $m/z = 29$ comprises a significant part of HCO^+.

By simply cleaving specific single bonds of the propanal molecule, the formation of the major fragment ions is easily explained. The rather intense parent ion peak points to a large fraction of stable molecular ions. However, interpreting the signals at $m/z = 30$ and at $m/z = 28$ needs somewhat more thought. The same straightforward cleavage procedure is less persuasive for allyl alcohol. It serves well to explain signals at $m/z = 57, 41, 31, 27$ but fails to account for most of the other peaks and, in particular, as compared with propanal, the practically reversed intensity ratio of $m/z = 58$ and $m/z = 57$. Using a simple bond-strength argumentation, the aldehyde hydrogen atom is much less tightly bound than its alcoholic counterpart as well as the aliphatic hydrogen atoms in the two molecules.

Table 1
Mass spectral data of propanal **(4)** and allyl alcohol **(2)**

		Propanal			Allyl alcohol
m/z	Ion	EI, 70 eV[a]		PI, 21.22 eV[b]	PI, 21.22 eV[c]
58	$C_3H_6O^+$	59		84	23
57	$C_3H_5O^+$	20		29	100
55	$C_3H_3O^+$	2		1	4
43	$C_2H_3O^+$	2			2
42	$C_2H_2O^+$	2			
41	$C_3H_5^+$	2			4
40	$C_3H_4^+$	1			6
39	$C_3H_3^+$	3			16
31	CH_3O^+	4		3	29
30	CH_2O^+			6	14
30	$C_2H_6^+$	4			
29	CHO^+	26	100	100	42
29	$C_2H_5^+$	74			
28	CO^+			61	13
28	$C_2H_4^+$	58			
27	$C_2H_3^+$	39		34	13
26	$C_2H_2^+$			2	1

[a] High resolution electron impact (EI) data drawn from [21].
[b] This work, contributions due to ^{13}C have been corrected for.
[c] See [11], contributions due to ^{13}C have been corrected for.

3.3. Fate of propanal cations with low internal energy ($E^* < 0.65$ eV)

$\mathbf{4}^+$ generated with little vibrational excitation in the electronic ground state cannot fragment for energetic reasons. Accordingly, only stable molecular ions

Table 2
Calculated 0 K threshold energies of some selected unimolecular reactions of propanal cation.[a]

Reaction	Products	0 K threshold energy
(1)	$\rightarrow CH_3CH_2CO^+$ [b] + H	10.31
(1')	$\rightarrow CH_2CHCHOH^+$ [c] + H	10.84
(1a)	$\rightarrow C_2H_5^+ + CO + H$	12.30
(2)	$\rightarrow C_2H_6^+ + CO$	11.40
(2')	$\rightarrow CH_2O^+ + C_2H_4$	12.18
(2a)	$\rightarrow C_2H_4^+ + CO + H_2$	11.74
(3)	$\rightarrow C_2H_5^+ + HCO$	11.69
(3')	$\rightarrow C_2H_3^+ + HCO + H_2$	13.56
(4)	$\rightarrow HCO^+$ [d] $+ C_2H_5$	11.67
(5)	$\rightarrow C_2H_4^+ + CH_2O$	11.83
(6)	$\rightarrow CO^+ + C_2H_6$	13.89
(7)	$\rightarrow C_2H_3^+ + H + CO + H_2$	14.18

[a] For the thermochemical data used, see Table 3. 0 K threshold energies are in eV.
[b] Propanoyl.
[c] Hydroxyallyl.
[d] Formyl.

are detected in coincidence with the corresponding photoelectrons. This makes it possible to unambiguously determine the absolute ion transmission coefficient $f_i(M^+)$ for thermal propanal cations. $f_i(M^+) = 0.20$ was obtained in perfect agreement with our earlier work on several other $C_3H_6O^+$ isomers [11,15] and the known transmission characteristics of our coincidence spectrometer. Based on this calibration, the parent ion branching ratio can be measured accurately at any other ionization energy. Inspecting Fig. 1, we note that the parent ion breakdown curve begins to decline at about 10.2 eV. Furthermore, the absolute flight-time of the detected parent ions is $\tau(M^+, m/z = 58) = 38\ \mu s$. When the thermal energy content of the neutral precursor, the transmission function of the electron energy analyzer and $\tau(M^+, m/z = 58)$ are all explicitly taken into account, the observed declining flank of the molecular ion breakdown curve can be fit perfectly. The outcome of this convolution and matching procedure are the 0 K threshold energy and a lower bound to the minimum rate of the least endothermic fragmentation reaction [cf. Table 2, reaction (1)]. In case of the former quantity we obtain $AE_{0\ K}$ ($CH_3CH_2CO^+ + H/\mathbf{4}$) = 10.56 + 0.15 eV, whereas the rate of this process must exceed $\sim 10^6\ s^{-1}$. Decay rates equal to or larger than this result would give rise to a sudden decrease (step-function behavior) of the parent ion breakdown curve in a hypothetical experiment at 0 K and infinite electron energy resolution.

As to this onset energy we like to point out that it is possibly biased toward lower energies, because of the specific course of the Franck-Condon factor for direct photoionization. Regarding the extent of this displacement at most a tenth of an electron volt is conceivable. Relative to the thermochemical limit (cf. Table 2) our value thus implies an activation energy barrier of $\geq$25 kJ/mol for the reverse ion-molecule reaction. This is in perfect accord with the calculated value of $\approx$30 kJ/mol [9]. A straightforward comparison with dissociative photoionization studies of propanal is hindered by several aspects. In an earlier publication, simply a threshold value of 10.79 eV was reported [13]. In a second article [14] the crucial part of the $C_3H_5O^+$ photoionization efficiency curve was depicted. This curve consists of two linear segments. The first one is of low slope with an indicated onset energy of 10.18 eV and extending for about half an electron volt. Then, at about 10.68 eV the curve experiences a sudden sharp increase. All this is rationalized in [14] as follows. Owing to its much higher inherent sensitivity and extremely long data acquisition periods, the low energy tailing with its threshold at 10.18 eV could be detected in the second study and a kinetic shift is invoked as its most likely explanation [14]. However, the origin and the significance of this dramatic change of slope around 10.68 eV is not explained. Most amazingly, we learn in the corresponding text of a sharp increase occuring at 10.78 eV, which is clearly incompatible with the data shown in Fig. 1 of [14]. Based on the ab initio molecular orbital calculations [9] neither an appearance energy as low as 10.18 eV nor a kinetic shift would be expected. The only way out suggested to bring measured and computed data in line was tunneling of the expelled hydrogen atom [9].

Our interpretation of the entire set of data assigns a decisive role to the nature of the ionization processes in, question. Supposing that the change of slope occurs at IE = 10.68 eV and bearing in mind

that our 0 K value of 10.56 eV is biased, we adopt this PI result determined at ambient temperatures as the experimental threshold for the formation of $CH_3CH_2CO^+$ + H. This is compatible with the calculated energy profile [9]. It also means that dissociation occurs when sufficiently excited vibrational levels of the ground state manifold are populated by direct photoionization. Whereas He-Iα PEPICO is limited to this latter process, dissociative PI also comprises autoionization of superexcited Rydberg states. It is conceivable that this latter way of initial excitation opens specific fragmentation pathways. In this manner, possibly by means of tunneling, a much lower threshold could be explained and even low rates giving rise to a kinetic shift seem possible. This could also account for the metastable signals observed in other studies [12]. However, the 10.18 eV are definitely too low and even in conflict with the established thermochemistry.

Concerning the rate energy function our results are in perfect accord with the outcome of [9]. Relying on quasi-equilibrium theory (QET [22]) and adopting the fundamentals of the neutral [23] we calculated a threshold rate of $\sim 5 \times 10^8$ s^{-1} based on an exact count algorithm [24]. Using the Stein-Rabinovitch [25] algorithm and scaled frequencies, a threshold rate of $\sim 2 \times 10^8$ s^{-1} was obtained in [9]. Moreover, it was found that this threshold rate is larger than 10^7 s^{-1} for any reasonable critical energy. Consequently, no metastable signals, let alone a significant kinetic shift, are to be expected. In general the predictive power of such calculated threshold rates stands and falls with the applicability of QET [22]. However, in the present case, the coincidence data provide an experimental lower bound of 10^6 s^{-1} implying no significant metastable signals and corroborating the calculated values [9].

3.4. Fate of propanal cations with high internal energy ($E^* > 0.65$ eV)

For the reasons specified we relied on the parent ion breakdown curve to determine the threshold energy of the least endothermic fragmentation (see Fig. 1). On turning our attention to the $C_3H_5O^+$ fragment ion data at IE $>$ 11.9 eV, we note a monotonously decreasing breakdown curve. Whereas at threshold the $C_3H_5O^+$ daughter ions must have the propanoyl structure (**a**, cf. Scheme 2), several other isomers are now energetically accessible, begining with hydroxyallyl cation (**b**, less stable by 51 kJ/mol [26], cf. Table 3) ring-opened oxetanyl (**c**, 149 kJ/mol [26]), oxetanyl (**d**, 157 kJ/mol [26]), methyl oxiranyl (**e**, 163 kJ/mol [26]), 2-hydroxyallyl (**f**, 183 kJ/mol [26]) and acetylmethylium (**g**, 318 kJ/mol [26]). Also, $C_3H_5O^+$ fragment ions can dissociate further according to reaction (1a) (cf. Table 2). This secondary decay has been shown to essentially proceed activation-energy free [27]. Strictly speaking, in any PEPICO experiment, only the parent ions are of defined internal energy. In good approximation, we may assume that this property is passed on to the propanoyl daughter ions as practically the entire excess energy of reaction (1) is likely to be stored in the internal degrees of freedom of the charged fragment. When the $C_3H_5O^+$ breakdown curve of the present work is compared with its counterpart for $\mathbf{2}^+$ and $\mathbf{3}^+$ [11], a substantial difference is noticed. In the case of $\mathbf{4}^+$ the $C_3H_5O^+$ branching ratio is considerably smaller at any internal energy and the striking plateau reported in our earlier work [11] is completely absent. As a matter of fact, the only features the two breakdown curves have in common are the threshold and the "disappearance energy". Our interpretation of these findings is that most of the $C_3H_5O^+$ fragment ions originally generated by photoionizing **4** retain the propanoyl structure at higher excitation energies, too. They contain correspondingly large internal energies and fragment quickly by expelling a CO molecule as soon as this secondary decay becomes energetically feasible [cf. Table 2, reaction (1a)]. On the other hand, $\mathbf{2}^+$ and $\mathbf{3}^+$ after isomerization to $\mathbf{1}^+$, are likely to form higher energetic $C_3H_5O^+$ species having less direct access to to the secondary fragmentation channel quoted. It has been demonstrated that hydroxyallyl, the most easily attainable $C_3H_5O^+$ daughter ion structure for $\mathbf{1}^+$, is stable at internal energies 1 eV above the thermochemical limit for CO extrusion [28]. Therefore, the coincidence data for $C_3H_5O^+$ prove that $\mathbf{4}^+$ does not at all or at most to a much

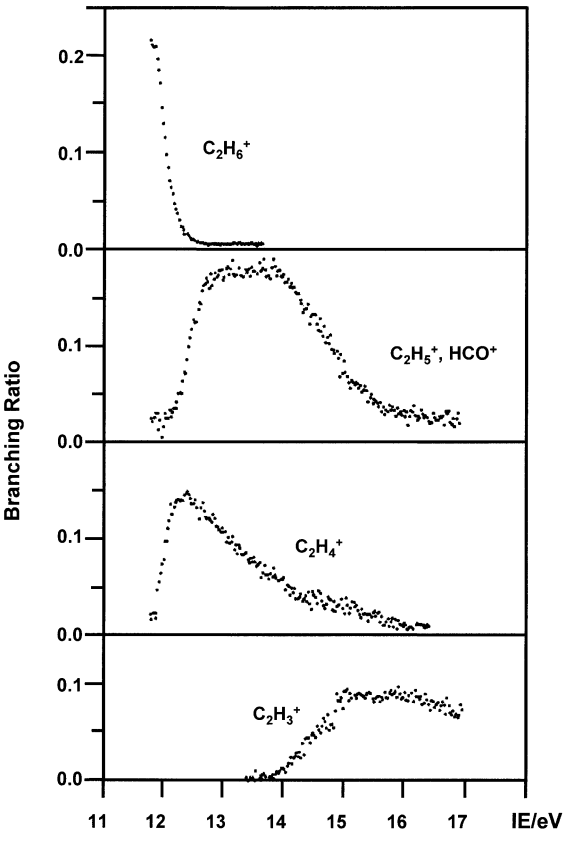

Fig. 2. Breakdown curves for the indicated fragment ions.

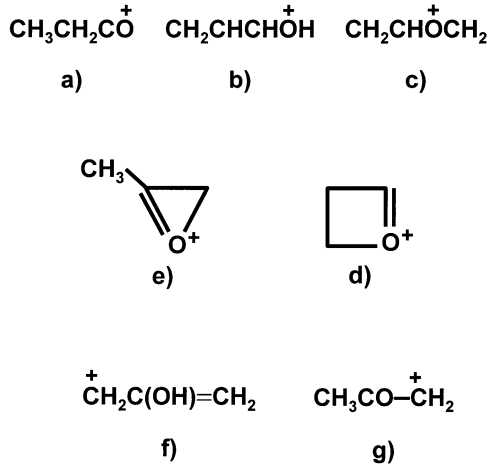

Scheme 2. Relevant $C_3H_5O^+$ fragment ion structures.

smaller extent isomerize to $\mathbf{1}^+$, as do $\mathbf{2}^+$ and $\mathbf{3}^+$. Note that this holds true for excitation energies of several electron volts. Distinctly different dissociation characteristics of $\mathbf{1}^+$ and $\mathbf{4}^+$ have been reported [10]. In relation to the mass spectrum of propanal the PEPICO data furnish a straightforward explanation for the surprisingly low relative intensity of the $C_3H_5O^+$ signal. The large Franck-Condon gap between the two lowest energetic double states and the rapid secondary decay of the predominantly formed propanoyl isomer are both responsible for this. In addition, the comparable relative intensities in the PI and EI mass spectrum (cf. Table 1) imply similar energy deposition function for both kinds of ionization. Consequently, it is appropriate to draw on both sorts of experiment to rationalize the fate of $\mathbf{4}^+$ as a function of its internal energy.

According to the high-resolution EI data [21] (cf. Table 1), the total signal intensity at $m/z = 30$ is due to $C_2H_6^+$ ions only. With a view to compare the fragmentation behavior of $\mathbf{1}^+$ and $\mathbf{4}^+$, we note that in the pertinent energy range direct PI of **4** yields the same $C_2H_6^+$ breakdown curve as reported earlier for **2** and **3**. To be more precise, this holds explicitly true for the declining flank only. The onset and the rising part could not be measured for $\mathbf{4}^+$, because they lie in the Franck-Condon gap between the lowest two doublet states of $\mathbf{4}^+$. Where data are available, the two breakdown curves concur and it is reasonable to conclude that the formation and the secondary decay of $C_2H_6^+$ is the consequence of one and the same process irrespective of the structure of the originally ionized molecule (**2** and **3** on the one hand, **4** on the other). At first glance such a congruency puzzles inasmuch as the $C_2H_6^+$ fragment ions are necessarily generated in the course of a complex rearrangement/dissociation process. There is a consistent interpretation of these findings which also lets us estimate to what extent $C_3H_6O^+$ cations of distinct descent probe the same volume of phase space. Within the frame of QET [22], it is not feasible to account for the breakdown curves of the only two significant fragment ions at low excitation energies, i.e. $C_3H_5O^+$ and $C_2H_6^+$. This is a consequence of both the substantially higher (>1 eV) critical energy (cf. Table 2) and the

Table 3
Relevant thermochemical data.[a]

Neutral				Cation	
$\Delta_f H^\circ_{298(g)}$	$\Delta_f H^\circ_{0(g)}$	$\Delta_f H^\circ_{298(g)}$	IE	$\Delta_f H^\circ_{0(g)}$	$\Delta_f H^\circ_{298(g)}$
C_3H_6O, **4**	−170.7[b]	−188.7[c]	9.96	790	772
CH_3CH_2CO			5.7	608[b]	591
$CH_2CHCHOH$				659[b]	642
C_2H_6	−68.24[b]	−83.85[d]	11.52	1043.2[b]	1027.6
CH_2O	−105.0[b]	−108.6[e]	10.87	943.6[b]	940.0
C_2H_5	131[b]	119[f]	8.117[g]	914[b]	902
CHO	43	43.514[h]	8.12	824	824
C_2H_4	60.731[b]	52.467	10.51	1075.5[b]	1067.0
CO	−113.801	−110.53[i]	14.01	1238.0[b]	1241.3
C_2H_3	299	299[f]	8.25[j]	1095	1095
H	216.003	217.998	13.598	1530	1530

[a] Using the stationary electron convention [33]. Data drawn from [17] in the absence of other citations. Enthalpies are in kJ/mol and ionization energies (IEs) in eV.
[b] Calculated from the corresponding 298 K value using the molecular frequencies and the approximate enthalpy function.
[c] See [34].
[d] See [35].
[e] See [36].
[f] See [37].
[g] See [38].
[h] See [39].
[i] See [40].
[j] See [41].

considerably tighter transition state for the $C_2H_6^+$ formation. These two drawbacks prevent the $C_2H_6^+$ formation from effectively competing with reaction (1). Moreover, the fact that experimental and thermochemical threshold for $C_2H_6^+$ formation coincide [11] and hence the absence of any competitive shift, points in the same direction. As to the nature of this non-QET [22] behavior, the following is conceivable. Subsequent to population of the first excited electronic state $\tilde{A}$, radiationless transitions to the ground state compete with an electronic predissociation. The former way of depleting the $\tilde{A}$ state in conformity with QET [22], yields $C_3H_5O^+$ fragment ions after more (**2** and **3**) or less **(4)** extensive isomerizations. Presumably the electronic predissociation results from an interaction with an excited state hypersurface that correlates with a $C_2H_6^+$ + CO dissociation limit. The initial "railway switch" partitions the originally generated parent ion population irrespective of the nature of the precursor molecule. Predissociating molecular ions yield $C_2H_6^+$, whereas those ending up on the ground state manifold randomize their internal energy and dissociate by H abstraction accompanied by more or less extensive isomerizations. The nature of the neutral precursor is mapped into this second fragmentation pathway. In terms of ease of fragmentation into propanoyl cation and a hydrogen atom, ionizing **4** is most favorable and, accordingly the formation of higher energetic $C_3H_5O^+$ isomers, is handicapped for kinetic reasons (vide supra). Starting out with **2** or **3** yields distonic ion $\mathbf{1}^+$ [9,10] which must rearrange to $\mathbf{4}^+$ prior to the formation of propanoyl fragment ions. On the other hand, when energetically accessible, $\mathbf{1}^+$ may decay into higher energetic $C_3H_5O^+$ species (e.g. hydroxyallyl) without any preceding isomerization.

Unfortunately, the ab initio computations have been confined to the ground state manifold and, in particular, calculated data on reaction (2) are lacking. However, there are alternative models to describe this formation of $C_2H_6^+$. One of them, put forward on reacting to our earlier study [11], suggests that extricating CO from $\mathbf{2}^+$ and $\mathbf{3}^+$ is initiated by a preceding isomerization to the carbene isomer [29]. Right or wrong, this proposal does not explain the apparent

lack of competition between the two dissociation pathways in question. In this context, the concept of ion–neutral complexes [30] and their decomposition behavior seems more useful. It renders it possible to simultaneously account for the coincidence data for $C_2H_6^+$ as well as those for $C_2H_4^+$ (vide infra).

Adopting the high-resolution EI data [21] (cf. Table 1) a quarter of the total intensity at *m/z* = 29 originates in HCO^+ whereas $C_2H_5^+$ contributes three times as much. Formation of daughter ions of *m/z* = 29 corresponds to breaking $\mathbf{4}^+$ into two pieces of equal mass number. The thermochemical limits for the two conceivable pairs of charged and neutral fragments fortuitously practically concur (cf. Table 2). They are located slightly below the onset of the second PE band. Effective competition in form of a primary fragmentation pathways of the parent ions is likely to contribute very little or not at all to the *m/z* = 29 breakdown curve, as hydrogen abstraction strongly dominates at this level of excitation. Most of the fragment ions of *m/z* = 29 stem from secondary decays of $C_3H_5O^+$ and $C_2H_6^+$ (vide infra). Again, comparison with our earlier data on $\mathbf{2}^+$ and $\mathbf{3}^+$ reveals significant differences. The *m/z* = 29 breakdown curve determined for $\mathbf{4}^+$ rises much more steeply and shows a strongly marked plateau region between 13 and 14 eV. Since the $C_2H_6^+$ supply channel is identical for all the three isomers $\mathbf{2}^+$, $\mathbf{3}^+$, and $\mathbf{4}^+$ (vide infra) the difference originates in the distinct $C_3H_5O^+$ fragment ion structures produced by the decay of $\mathbf{1}^+$ and $\mathbf{4}^+$, respectively, as discussed previously. The strongly dominant propanoyl isomer in the case of $\mathbf{4}^+$ represents a precursor with a rather limited spread of internal energies, which is in line with the bigger slope of the rising flank of the *m/z* = 29 breakdown curve. The decline of the *m/z* = 29 breakdown curve, which sets in at IE ≈ 14 eV is accompanied by a correspondingly rising $C_2H_3^+$ branching ratio. This implies subsequent dissociation of sufficiently excited $C_2H_5^+$ fragment ions by loss of a hydrogen molecule. It should be noted that the *m/z* = 29 breakdown curve does not completely drop to zero in the energy range investigated. We attribute the remaining intensity above 16 eV exclusively to CHO^+ ions, which resist any secondary decay in the energy range considered [31].

We conclude the discussion of the breakdown diagram of $\mathbf{4}^+$ with some comment on $C_2H_4^+$. All the results adduced to uncover the non-statistical nature of $C_2H_6^+$ formation prove even more appropriate for $C_2H_4^+$. Reactions (2a) and (5) are even more handicapped than reaction (2) respecting competition with reaction (1). Therefore, in the first instance, the $C_2H_4^+$ fragment ion is regarded as a secondary decay product of $C_2H_6^+$. The breakdown diagram of the latter is well known. It was determined quite some time ago [32]. Indeed, $C_2H_6^+$ preferentially decays by loss of molecular hydrogen at low excitation energies. Also, concomitant production of $C_2H_5^+$ is in line with our breakdown data. However, when compared with the corresponding data for $\mathbf{2}^+$ and $\mathbf{3}^+$, it is noticed that substantially more $C_2H_4^+$ is formed in the case of $\mathbf{4}^+$. To account for this difference we like to draw again on the quoted concept of ion–neutral complexes [30]. A conceivable complex of this kind was suggested to rationalize the formation of $C_2H_6^+$. The sequence proposed [10] was

$$\mathbf{1}^+ \rightarrow C_2H_4/CHOH^+\cdot \rightarrow C_2H_6^+\cdot/CO \rightarrow C_2H_6^+\cdot + CO$$

Likewise, $C_2H_4^+$ could be generated. Typically formation of such ion–neutral complexes becomes possible somewhat below the thermochemical limit of the separated fragments, depending on their binding energy.

To sum it up, the production of $C_2H_6^+$ fragment ions is independent of the precursor molecule (**2**, **3**, or **4**) and of non-statistical nature in the sense of the QET [22]. The formation of $C_2H_4^+$, much enhanced in the case of $\mathbf{4}^+$ as compared with $\mathbf{2}^+$ and $\mathbf{3}^+$, may emanate directly from an initial ion–neutral complex or, at least in parts, be a secondary decay product of $C_2H_6^+$. The cited difference shows that regarding $C_2H_4^+$, the $C_3H_6O^+$ isomers in question behave differently.

4. Conclusions

He-Iα PEPICO remains a preferential technique to study the behavior of internal energy selected ions. It

provides energy-, mass- and even time-resolved breakdown diagrams of radical cations over several electron volts of excitation energy and excels in this way as a most valuable source of experimental data. Whereas its "blindness" in Franck-Condon gaps and its rather limited energy resolution are rightly considered to be of disadvantage, its capability to provide data practically unaffected by autoionization is fairly exceptional. This makes it possible to reveal a conceivable role of the nature of the initial ionization process on the determination of appearance energies. This could account for a much lower threshold energy of the least endothermic fragmentation of propanal cation in a PI experiment, although the reported 10.18 eV [14] are definitely too low. At this energy, the high PE signal intensity and a parent ion flight time of almost 40 μs would warrant the detection of such a dissociation threshold in our experiments. However, based on a proven way of analyzing the molecular ion breakdown curve, we derived a 0 K appearance energy of $>10.56 \pm 0.15$ eV, which is in accord with the ab initio calculated energy profile along the reaction coordinate. Moreover, the coincidence data exclude a significant kinetic shift occurring over several tenths of an electron volt of excitation energy.

In accord with various theoretical and experimental investigations our data confirm that propanal cation essentially retains its structure when generated with up to a few tenths of an electron volt of excitation. Also, in this energy range the $C_3H_5O^+$ fragment ion has the propanoyl structure. The corresponding breakdown curve implies that this very fragment ion structure prevails at higher ionization energies, too. Our breakdown diagram also explains the surprisingly low intensity of the $m/z = 57$ peak in the mass spectrum of propanal. It is a consequence of both the Franck-Condon gap between the lowest two doublet states of the propanal radical cation and of the absence of kinetically stable $C_3H_5O^+$ species isomeric to propanoyl cation. Owing to very similar energy deposition functions, He-Iα PEPICO data are quite generally most relevant to conventional EI mass spectroscopy. When combined with QET calculations noncompeting dissociation reactions can be identified. In the case of propanal this concerns the processes leading to $C_2H_6^+$ and, in parts also, the one yielding $C_2H_4^+$. Electronic predissoociations and/or neutral–ion complexes are likely models to describe the formation of these small hydrocarbon cations. Further work is required to confirm or reject these interpretations of the data.

Acknowledgements

The authors recall with pleasure and gratitude the time when Edgar Heilbronner was heading the Physical-Chemistry Institute. He was teaching both science and leadership and filled the institute with a unique spirit. The authors wish Edgar a wonderful birthday and we should like to thank him once again for his generosity and his open-minded manner to handle all kinds of matters, opportunities, as well as problems.

References

[1] J.P. Maier, Mass Spectrom. Rev. 11 (1992) 119; E.J. Bieske, J.P. Maier, Chem. Rev. 93 (1993) 2603; D.A. Kirkwood, M. Tulej, M.V. Pachkov, M. Schnaiter, F. Guthe, M. Grutter, M. Wyss, J.P. Maier, G. Fischer, J. Chem. Phys. 111 (1999) 9280.
[2] H.M. Rosenstock, K. Draxl, B.W. Steiner, J.T. Herron, J. Phys. Chem. Ref. Data 6 Suppl. 1 (1977).
[3] K.-M. Weitzel, Ber. Bunsenges. Phys. Chem. 102 (1998) 989.
[4] T. Baer, P.M. Mayer, J. Am. Soc. Mass Spectrom. 8 (1997) 103; J. Laskin, J. Futrell, J. Phys. Chem 104 (2000) 5484.
[5] J.P. Maier, in Kinetics of Ion Molecule Reactions, P. Ausloos (Ed.), Plenum, New York, 1979; M. Allan, J. Dannacher, J.P. Maier, J. Chem. Phys. 73 (1980) 3114.
[6] W. Forst, Theory of Unimolecular Reactions, Academic, New York, 1973.
[7] H.M. Rosenstock, J. Dannacher, J.F. Liebman, Radiat. Phys. Chem. 20 (1982) 7; L.M. Duffy, J.W. Keister, T. Baer, J. Phys. Chem. 99 (1995) 17862; T. Baer, O.A. Mazyar, J.W. Keister, W. Jeffrey, P.M. Mayer, Ber. Buns. Ges. 101 (1997) 478.
[8] W.J. Bouma, J.K. MacLeod, L. Radom, J. Am. Chem. Soc. 102 (1980) 2246; C.E. Hudson, D.J. McAdoo, Org. Mass Spectrom. 17 (1982) 366; M. Gu, F. Turecek, ibid. 29 (1994) 85.
[9] G. Bouchoux, A. Luna, J. Tortajada, Int. J. Mass Spectrom. Ion Processes 55 (1983/1984)47.
[10] M.J. Polce, C. Wesdemiotis, J. Am. Soc. Mass Spectrom. 7 (1996) 573.
[11] R. Bombach, J. Dannacher, E. Honegger, J.-P. Stadelmann, R. Neier, Chem. Phys. 82 (1983) 459.

[12] J.L. Holmes, P.C. Burgers, Y.A. Mollah, Org. Mass Spectrom. 17 (1982) 127; Y. Hoppilliard, G. Bouchoux, P. Jaudon, Nouv. J. Chim. 6 (1982) 43; F. Turecek, V. Hanus, T. Gäumann, Int. J. Mass Spectrom. Ion Processes 69 (1986) 217.
[13] R.H. Staley, R.D. Wieting, J.L. Beauchamp, J. Am. Chem. Soc. 99 (1977) 5964.
[14] J.C. Traeger, Org. Mass Spectrom. 20 (1985) 223.
[15] J.-P. Stadelmann, Chem. Phys. Lett. 89 (1982) 174; R. Bombach, J.-P. Stadelmann, J. Vogt, Chem. Phys. 72 (1982) 259.
[16] J. Dannacher, Org. Mass Spectrom. 19 (1984) 253.
[17] S.G. Lias, J.E. Bartmess, J.F. Liebman, J.L. Holmes, R.D. Levin, W.G. Mallard, J. Phys. Chem. Ref. Data 7 Suppl. (1988).
[18] K. Kimura, S. Katsumata, T. Yamazaki, H. Wakabyashi, J. Electron Spectrosc. Relat. Phenom. 6 (1975) 41.
[19] W.C. Tam, D. Yee, C.E. Brion, J. Electron Spectrosc. Relat. Phenom. 4 (1974) 77.
[20] R. Hernandez, P. Masclet, G. Mouvier, J. Electron Spectrosc. Relat. Phenom. 10 (1977) 333.
[21] A.G. Harrison, Org. Mass Spectrom. 3 (1970) 549.
[22] H.M. Rosenstock, M.B. Wallenstein, A.L. Wahrhaftig, H. Eyring, Procl. Natl. Acad. Sci. U.S.A. 38 (1952) 667.
[23] S.G. Frankiss, W. Knyasto, Spectrochim. Acta A 28 (1972) 2149.
[24] T. Beyer, D.F. Swinehart, ACM Commu. 16 (1973) 379.
[25] S.E. Stein, B.S. Rabinovitch, J. Chem. Phys. 58 (1973) 2438.
[26] G. Bouchoux, J.-P. Flament, Y. Hoppilliard, Nouv. J. Chim. 9 (1985) 453; G. Bouchoux, J.-P. Flament, Y. Hoppilliard, ibid. 7 (1983) 385.
[27] R.D. Bowen, D.H. Williams, J. Chem. Res. (S) 12 1978, 482.
[28] G. Bouchoux, Y. Hoppilliard, Int. J. Mass Spectrom. Ion Phys. 47 (1983) 105.
[29] D.J. McAdoo, C.E. Hudson, J.C. Traeger, Int. J. Mass Spectrom. Ion Processes 79 (1987) 183.
[30] T.H. Morton, Tetrahedron 38 (1982) 3195; D.J. McAdoo, J. Mass Spectrom. Rev. 7 (1988) 363.
[31] R. Bombach, J.-P. Stadelmann, J. Vogt, Int. J. Mass Spectrom. Ion Phys. 40 (1981) 275.
[32] R. Stockbauer, J. Chem. Phys. 58 (1973) 3800; R. Bombach, J. Dannacher, J.-P. Stadelmann, Int. J. Mass Spectrom. Ion Phys. 58 (1984) 217.
[33] H.M. Rosenstock, in Kinetics of Ion Molecule Reactions, P. Ausloos (Ed.), Plenum, New York, 1979, p. 246.
[34] K.B. Wiberg, L.S. Crocker, K.M. Morgan, J. Am. Chem. Soc. 113 (1991) 3447.
[35] D.A. Pittam, G. Pilcher, J. Chem. Soc. Faraday Trans. 1 68 (1972) 2224.
[36] R.A. Fletcher, G. Pilcher, Trans. Faraday Soc. 66 (1970) 794.
[37] W. Tsang, Heats of Formation of Organic Free Radicals by Kinetic Methods in Energetics of Organic Free Radicals, J.A. Martinho Simoes, A. Greenberg, J.F. Liebman (Eds.) Blackie Academic and Professional, London, 1996, p. 22.
[38] B. Ruscic, J. Berkowitz, L.A. Curtiss, J. Chem. Phys. 91 (1989) 114.
[39] M.W. Chase Jr., NIST-JANAF Thermochemical Tables, fourth edition, J. Phys. Chem. Ref. Data, Monograph 9, 1998, p. 1.
[40] J.D. Cox, D.D. Wagman, V.A. Medvedev, CODATA Key Values for Thermodynamics, Hemisphere, New York, 1984, p. 1.
[41] J.A. Blush, P.J. Chen, J. Phys. Chem. 96 (1992) 4138.